Oxidized Ruthenium Ferrocenylacetylide Complexes, [(η-C5H5)L2RuCCFc]PF6 and [(η-C5Me5)L2RuCCFc]PF6 (L = Phosphines). Electron-Delocalized Heterobinuclear Mixed-Valence Complexes

Masaru Sato,* Hitoshi Shintate, Yasushi Kawata, and Masato Sekino

Chemical Analysis Center, Saitama University, Urawa, Saitama 338, Japan

Motomi Katada and Satoshi Kawata

*Department of Chemistry, Faculty of Science, Tokyo Metropolitan University,
Hachioji, Tokyo 192-03, Japan*

Received April 14, 1993[⊛]

The reaction of ferrocenylacetylene with $(\eta\text{-C}_5R_5)L_2RuCl$ [R = H or Me; L_2 = 2PPh$_3$, Ph$_2$-PCH$_2$CH$_2$PPh$_2$ (dppe), or (Ph$_2$PC$_5$H$_4$)$_2$Fe (dppf)] in the presence of NH$_4$PF$_6$ and the subsequent treatment with alkali gave ruthenium(II) ferrocenylacetylide complexes $(\eta\text{-C}_5R_5)L_2RuCCFc$ in good yields. Cyclic voltammetric data suggest the large electron delocalization between the Fe atom of the ferrocene moiety and the Ru(II) atom in their one-electron-oxidized complexes. The IR spectra of the oxidized ferrocenylacetylide complexes and the molecular structure of $[(\eta\text{-C}_5H_5)(\text{Ph}_3P)_2Ru(CCFc)]PF_6$ determined by X-ray diffraction gave an evidence for such electron delocalization. Crystallographic data for **12** are as follows: space group $P2_1/a$, a = 17.176(9) Å, b = 12.055(7) Å, c = 22.480(9) Å, β = 101.35(4)°, V = 4563(4), Z = 4. The complexes showed low-energy absorption bands assigned to intervalence transfer transitions in the near-infrared (NIR) region. The parameter α^2, which shows the degree of ground-state delocalization in a mixed-valence complex, is almost as large as that in the [0.0] ferrocenophane monocation. The NIR spectrum, along with the Mössbauer spectra, suggest that the oxidized acetylide complexes are a well electron-delocalized class II type of a heterobinuclear mixed-valence complex.

The compounds involving the different redox sites in close proximity often exhibit physical properties which may be characteristic of a particular compound, rather than a sum of the properties of the individual redox sites. Mixed-valence compounds are of great interest from the viewpoints of producing high temperature superconducting materials and new semiconducting materials and of understanding biologically relevant mixed-valence compounds.[1] In the field of organometallic mixed-valence complexes, oxidized species of binuclear ferrocene derivatives have been intensively investigated in relation to the mixed-valence state[2-6] and also applied to a polymeric mixed-valence system[7] and a regularly orientated mixed-valence complex in monolayer assemblies.[8] A hetero-

nuclear organometallic compound showing mixed-valence-like properties was also synthesized in order to get more insight into the electronic structure of mixed-valence compounds, the factors affecting electron transfer between interacting sites, and the extent of delocalization of the valence electrons. Thus, the oxidation reactions of several ferrocene derivatives involving another transition metal as one component have been investigated by electronic spectroscopy[9-11] and cyclic voltammetry.[9-16] Several interesting heteronuclear-bimetallic complexes are also reported,[17-23] inclusive of the trinuclear ruthenium acetylide complex.[24] We now report the first isolation and

[⊛] Abstract published in *Advance ACS Abstracts*, April 1, 1994.

(1) Brown, D. B., Ed. *Mixed-Valence Compounds*; D. Reidel Publishing Co.: Dordrecht, Holland, 1980.

(2) (a) Cowan, D. O.; Kaufman, F. *J. Am. Chem. Soc.* 1970, *92*, 219. (b) Kaufman, F.; Cowan, D. O. *J. Am. Chem. Soc.* 1970, *92*, 6198. (c) Cowan, D. O.; LeVanda, C.; Park, J.; Kaufman, F. *Acc. Chem. Res.* 1973, *6*, 1.

(3) (a) Cowan, D. O.; LeVanda, C. *J. Am. Chem. Soc.* 1972, *94*, 9271. (b) Mueller-Westerhoff, U. T.; Eilbracht, P. *J. Am. Chem. Soc.* 1972, *94*, 9272. (c) LeVanda, C.; Bechgaard, K.; Cowan, D. O.; Mueller-Westerhoff, U. T.; Eilbracht, P.; Candela, G. A.; Collins, R. L. *J. Am. Chem. Soc.* 1976, *98*, 3181. (d) Morrison, W., Jr.; Krogsrud, S.; Hendrickson, D. N. *Inorg. Chem.* 1973, *12*, 1998.

(4) (a) LeVanda, C.; Bechgaard, K.; Cowan, D. O. *J. Org. Chem.* 1976, *41*, 2700. (b) Motoyama, I.; Watanabe, M.; Sano, H. *Chem. Lett.* 1978, 513. (c) Kramer, J. A.; Hendrickson, D. N. *Inorg. Chem.* 1980, *19*, 3330. (d) Powers, M. J.; Meyer, T. J. *J. Am. Chem. Soc.* 1978, *100*, 4393.

(5) Amer, S. I.; Sadler, G.; Henry, P. M.; Ferguson, G.; Ruhl, B. L. *Inorg. Chem.* 1985, *24*, 1517.

(6) Lee, M.-T.; Foxman, B. M.; Rosenblum, M. *Organometallics* 1985, *4*, 539.

(7) Pittmann, C. U., Jr.; Surynarayanan, B. *J. Am. Chem. Soc.* 1974, *96*, 7916.

(8) Sato, M.; Nakahara, H.; Fukuda, S.; Akabori, S. *J. Chem. Soc., Chem. Commun.* 1988, 24.

(9) (a) Dowling, N.; Henry, P. M.; Lewis, N. A.; Taube, H. *Inorg. Chem.* 1981, *20*, 2345. (b) Dowling, N.; Henry, P. M. *Inorg. Chem.* 1982, *21*, 4088.

(10) Colbran, S. B.; Robinson, B. H.; Simpson, J. *Organometallics* 1983, *2*, 943, 952.

(11) Kotz, J. C.; Getty, E. E.; Lin, L. *Organometallics* 1985, *4*, 610.

(12) Diaz, A. F.; Mueller-Westerhoff, U. T.; Nazzal, A.; Tanner, M. *J. Organomet. Chem.* 1982, *236*, C45.

(13) Kotz, J.; Neyhart, G.; Vining, W. J.; Rausch, M. D. *Organometallics* 1983, *2*, 79.

(14) Clemente, D. A.; Pilloni, G.; Corain, B.; Longato, B.; Tiripicchio-Camellini, M. *Inorg. Chim. Acta* 1986, *115*, L9.

(15) (a) Schwarzhaus, K. E.; Shottenberg, H. *Z. Naturforsch.* 1983, *38B*, 1493. (b) Obendorf, D.; Schottenberger, H.; Rieker, C. *Organometallics* 1991, *10*, 1293.

(16) Kasahara, Y.; Hoshino, Y.; Kajitani, M.; Shimizu, K.; Sato, G. P. *Organometallics* 1992, *11*, 589.

(17) (a) Casey, C. P.; Bullock, R. M.; Fultz, W. C.; Rheingold, A. L. *Organometallics* 1982, *1*, 1591. (b) Doyle, M. J.; Duckworth, T. J.; Manojlovic-Muir, L.; Mays, M. J.; Raithby, P. R.; Robertson, F. J. *J. Chem. Soc., Dalton Trans.* 1992, 2703.

(18) Sterzo, C. L.; Stille, J. K. *Organometallics* 1990, *9*, 687. Sterzo, C. L. *Organometallics* 1990, *9*, 3185.

characterization of the stable oxidized ferrocenylacetylide complexes showing high delocalization of the valence electron.

RuCl(PPh$_3$)$_2$(η-C$_5$H$_5$) (1) reacted with ferrocenylacetylene in the presence of NH$_4$PF$_6$ in methanol and subsequently was chromatographed on alumina to give the corresponding acetylide complex 4 in 94% yield. From

1 P, P=2PPh$_3$
2 P, P=dppe
3 P, P=dppf

4 P, P=2PPh$_3$
5 P, P=dppe
6 P, P=dppf
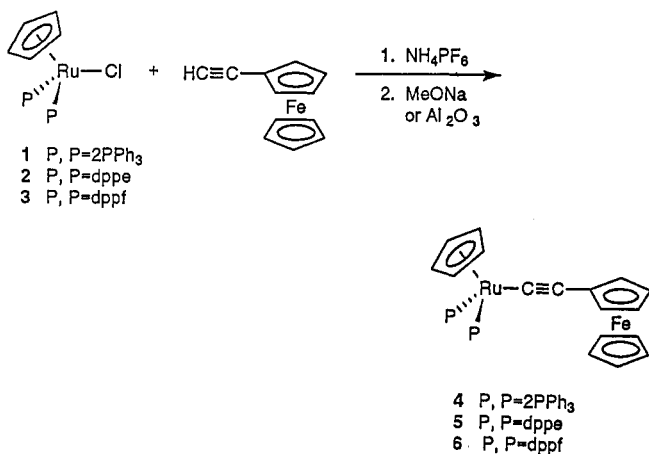
RuCl(dppe)(η-C$_5$H$_5$) (2) [dppe = 1,2-bis(diphenylphosphino)ethane] and RuCl(dppf)(η-C$_5$H$_5$) (3) [dppf = 1,1'-bis(diphenylphosphino)ferrocene], the corresponding ferrocenylacetylide complexes 5 and 6 were similarly obtained in good yields, respectively. The permethylcyclopentadienyl analogs 7 and 8 were prepared in a similar manner.

7 P, P=2PPh$_3$
8 P, P=dppe
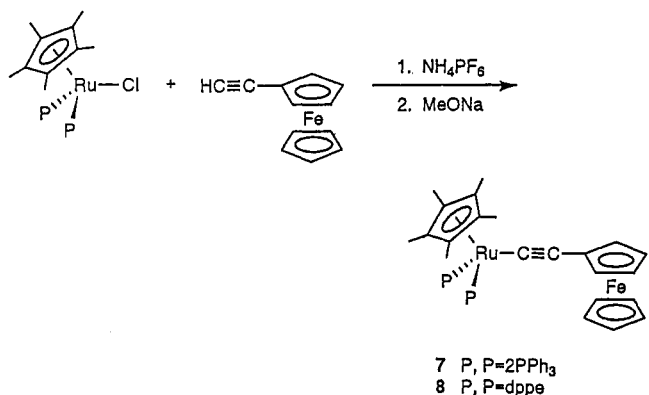
The structures of 4–8 were assigned by the IR, ^{1}H, and ^{13}C NMR spectra and elemental analyses. For example, the IR spectrum of 5 showed the C–C stretching absorption at 2076 cm^{-1}. In the ^{1}H NMR spectrum of 5, the α, β, and unsubstituted ring protons in the ferrocene moiety were observed at δ 3.71, 3.48, and 3.64, respectively. The protons of the cyclopentadienyl ligand coordinated to the Ru(II) atom resonated at δ 4.72. The methylene protons of dppe appeared at δ 2.39 and 2.82 as multiplets.

(19) (a) Bullock, R. M.; Lemke, F. R.; Szalda, D. J. *J. Am. Chem. Soc.* **1990**, *112*, 3244. (b) Lemke, F. R.; Szalda, D. J.; Bullock, R. M. *J. Am. Chem. Soc.* **1991**, *113*, 8466.

(20) Frank, K. G.; Selegue, J. P. *J. Am. Chem. Soc.* **1990**, *112*, 6414.

(21) van Rooyen, P. H.; Schindehutte, M.; Lotz, S. *Organometallics* **1992**, *11*, 1104. Lotz, S.; Schindehutte, M.; van Rooyen, P. H. *Organometallics* **1992**, *11*, 629.

(22) Herberhold, M.; Feger, W.; Kölle, U. *J. Organomet. Chem.* **1992**, *436*, 333.

(23) Baird, G. J.; Davis, S. G.; Moon, S. D.; Simpson, S. J.; Jones, R. H. *J. Chem. Soc., Dalton Trans.* **1985**, 1479.

(24) Koridze, A. A.; Yanovsky, A. I.; Struchkov, Y. T. *J. Organomet. Chem.* **1992**, *441*, 277.

Table 1. Redox Potentials (V) of Complexes 4–11 in 0.1 M Bu$_4$NClO$_4$–CH$_2$Cl$_2$ at 100 mV s^{-1} (vs FcH/FcH$^+$)[a]

compd	$E_{1/2}$ (1)	E_{pc} (2)	E_{pa} (2)
4	-0.31		+0.29
5	-0.34	+0.17	+0.30
6[b]	-0.33	+0.16	+0.38
7	-0.54	+0.16	+0.29
8	-0.55	-0.04	+0.15
9	+0.15		
10		-0.05	+0.05
11		-0.01	-0.20

[a] FcH/FcH$^+$ = +0.18 V vs Ag/Ag$^+$. [b] Additional peaks: E_{pc}(3) +0.45 V, E_{pa}(3) +0.59 V.
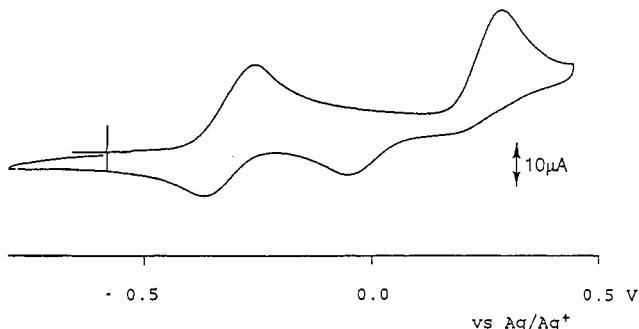
Figure 1. Cyclic voltamogram of 4 (10^{-3} M) vs Ag/Ag$^+$ in 0.1 M Bu$_4$NClO$_4$/CH$_2$Cl$_2$ at 100 mV s^{-1}.

The cyclic voltammograms of complexes 4–8, ferrocenylacetylene (9), (η-C$_5$H$_5$)(Ph$_3$P)$_2$RuCCPh (10), and (η-C$_5$Me$_5$)(Ph$_3$P)$_2$RuCCPh (11) were measured in 0.1 M [(C$_4$H$_9$)$_4$N]ClO$_4$/CH$_2$Cl$_2$ at room temperature, and the results are summarized in Table 1. The cyclic voltammogram of complex 4 is shown in Figure 1, in which a quasi-reversible wave [E_{pa}(1) – E_{pc}(1) = ca. 120 mV for 100 mV/s of scan rate] appeared at $E_{1/2}$(1) = -0.31 V and an irreversible wave at E_{pa}(2) = +0.29 V. An additional wave was observed at E_{pc} = -0.05 V, but this wave did not appear when the scanning turned back at +0.10 V. So, the wave seems to be due to the instability of the two-electron-oxidized species of 4, if the fact that the cathodic wave [E_{pc}(2)] corresponding to E_{pa}(2) is small or vanishing is taken into consideration. In complexes 5–8 one quasi-reversible and one irreversible waves were also observed. Complex 6 showed an additional wave due to the dppf moiety. The assignment of the waves observed in complexes 4–8 to the redox reaction of a particular metal center could not be definitely accomplished by comparison with the redox potentials of the reference compounds 9–11 because 9–11 afforded their redox waves in a similar potential region. It was unambiguously assigned from the result of the Mössbauer spectra that the low-potential wave was due to the Fe(II)/Fe(III) couple of the ferrocenyl moiety in complexes 4–8 (*vide infra*). The redox potential [$E_{1/2}$(1)] of the low-potential wave in 4–8 is considerably lower than that of ferrocenylacetylene. This is probably because the (η-C$_5$H$_5$)(PPh$_3$)$_2$Ru group is strongly electron-donating.[25] By using the correlation relationship proposed by Hoh et al.,[26] a value of -0.81 was, for example, calculated as the Hammett σ_p constant for the (η-C$_5$H$_5$)(Ph$_3$P)$_2$Ru group, whose value is closely similar to that (σ_p = -0.83) for a dimethylamino group which is the most electron-donating substituent. Replacement of the η-C$_5$H$_5$ ligand by the η-C$_5$Me$_5$ ligand on the Ru(II) atom of complex 4

(25) Bruce, M. I.; Wallis, R. C. *Aust. J. Chem.* **1979**, *32*, 1471.

(26) Hoh, G. L. K.; McEwen, W. E.; Kleinberg, J. *J. Am. Chem. Soc.* **1961**, *83*, 3949.

also brings about the shift of $E_{1/2}(1)$ to a low potential. This may reflect an increase of electron density on the Ru atom due to the permethylated cyclopentadienyl ligand. The oxidation potential [$E_{pa}(2)$] in 4–8 is observed at a potential higher by ca. 250 mV than that of the reference complexes 10 and 11. The shift to a higher potential is expected to take place as a result of the electrostatic effect by connection with the Fe(III) center through the C≡C bond in the molecule. This also suggests that the one-electron-oxidized species of complexes 4–8 is stabilized by electron delocalization between the two metal atoms.

Complexes 4–8 were oxidized with FcH⁺PF₆⁻ in dichloromethane/benzene at 0 °C. The oxidized species 12–14

4. P,P = 2PPh₃
6. P,P = dppf

12. P,P = 2 PPh₃
13. P,P = dppf

7. P,P = 2PPh₃

14. P,P = 2PPh₃
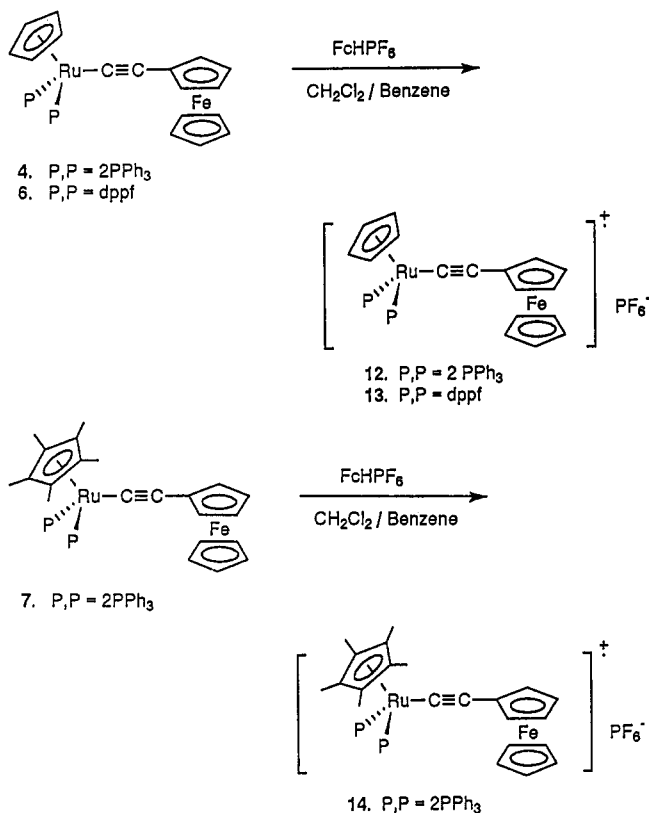
were black fine crystals and considerably stable in the solid state. But the acetylide complexes involving dppe as a phosphine ligand, 5 and 8, gave no stable and pure product, although they were oxidized. The IR spectra of 12–14 showed an intense absorption at 1986, 1972, and 1978 cm⁻¹, respectively, the position of which was intermediate between the absorption for the C≡C stretching vibration of the acetylide complex ($\sim$2070 cm⁻¹) and that for the =C=C= stretching vibration of the allenylidene complex (1926 cm⁻¹).[27] The IR spectral data suggest a large conjugation between the RuL₂(η-C₅H₅) part and the ferrocenyl part in the oxidized complexes. That is, the limiting structure **B**, being a type of allenylidene complex,

A   B
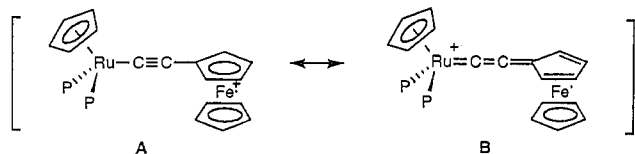
seems to play an important role in addition to the limiting structure **A** in the oxidized complex 12 (also probably in 13 and 14).

Table 2. Crystal and Intensity Collection Data for 12

mol formula	$C_{53}H_{44}P_3F_6RuFe$
mol wt	1044.76
cryst syst	monoclinic
space group	$P2_1/a$ (No. 14)
a, Å	17.176(9)
b, Å	12.055(7)
c, Å	22.480(9)
β, deg	101.35(4)
V, Å³	4365(4)
Z	4
D_{calc}, g cm⁻³	1.520
cryst dimens, mm	0.100 × 0.030 × 0.100
linear abs coeff, cm⁻¹	8.05
radiation (λ, Å)	Mo Kα (0.710 69)
2θ range, deg	8.6–23.5
scan type	$2\theta/\omega$
total no. of rflns scanned	5255
no. of unique rflns	4792 (R_{int} = 0.501)
no. of obsd rflns	1462 [$I > 3.00\sigma(I)$]
no. of variables	313
R	0.057
R_w	0.056
max peak in final diff map, e Å⁻³	+0.44
min peak in final diff map, e Å⁻³	−0.44

A single crystal X-ray diffraction study was undertaken to define the structure of complex 12. The crystallographic data and the position parameters are listed in Tables 2 and 3, respectively. The ball-and-stick formulation is shown in Figure 2, along with the selected numbering of the atoms. The selected bond lengths and bond angles are summarized in Table 4. The Ru–P distances [2.293-(7) and 2.303(7) Å] are almost similar to those of the neutral Ru acetylide complexes, e.g. 2.285(3) and 2.300(3) Å in [(η-C₅H₅)(Ph₃P)₂Ru(CCC(OCOCF₃)CMe₂)][28] and 2.285-(1) and 2.303(1) Å in [(η-C₅H₅)(Ph₃P)₂RuCCPh].[29] In general, the Ru—P bond in neutral Ru complexes is slightly shorter (by 0.02–0.04 Å) than that in cationic Ru complexes.[28,30,31] This means probably that the positive charge is considerably biased on the ferrocenium part in complex 12. The features observed in the ferrocenylacetylide ligand are noteworthy. The acetylide framework remains nearly linear [Ru—C(42)—C(43) 173(2)° and C(42)—C(43)—C-(44) 178(3)°]. The Ru—C(42) distance is 1.99(2) Å, which is slightly shorter than the typical Ru—C(sp) distance [e.g. 2.02(1) Å in (η-C₅H₅)(Ph₃P)₂Ru(CCC(OCOCF₃)-CMe₂),[28] 2.016(3) Å in (η-C₅H₅)(Ph₃P)₂RuCCPh,[29] and 2.017(9) Å in (η-C₅H₅)(Ph₃P)₂Ru(CCPh·CuCl)[32]] and is considerably longer than the Ru=C distance (1.845(7) Å) of the vinylidene complex {e.g. 1.812(9) Å in [(η-C₅H₅)(Ph₃P)₂Ru(CC(COCF₃)C(OCOCF₃)CMe₂)]⁺[28] and 1.863(10) Å in (η-C₅H₅)(Ph₃P)₂Ru(CCMePh)]PF₆[33]} or that (1.884 Å) in the allenylidene complex [(η-C₅H₅)(Me₃P)₂-Ru(CCCPh₂)]PF₆.[27] The C(42)–C(43) distance (1.19 Å) remains in the range for C≡C bond lengths in metal acetylide complexes (1.18–1.24 Å).[34] It is also worthy to note that the C(43)—C(44) distance is considerably shortened (1.38 Å) as a single bond. Moreover, some noticeable changes are observed in the ferrocenyl moiety:

(27) Selegue, J. P. *Organometallics* **1982**, *1*, 217.

(28) Lomprey, J. R.; Selegue, J. P. *Organometallics* **1993**, *12*, 616.

(29) Wisner, J. M.; Bartczak, T. J.; Ibers, J. A. *Inorg. Chim. Acta* **1985**, *100*, 115.

(30) Bruce, M. I.; Wong, F. S.; Skelton, B. W.; White, A. H. *J. Chem. Soc., Dalton Trans.* **1982**, 2203.

(31) Consiglio, G.; Morandini, F.; Sironi, A. *J. Organomet. Chem.* **1986**, *306*, C45. Consiglio, G.; Morandini, F.; Ciani, G. F.; Sironi, A. *Organometallics* **1986**, *5*, 1976.

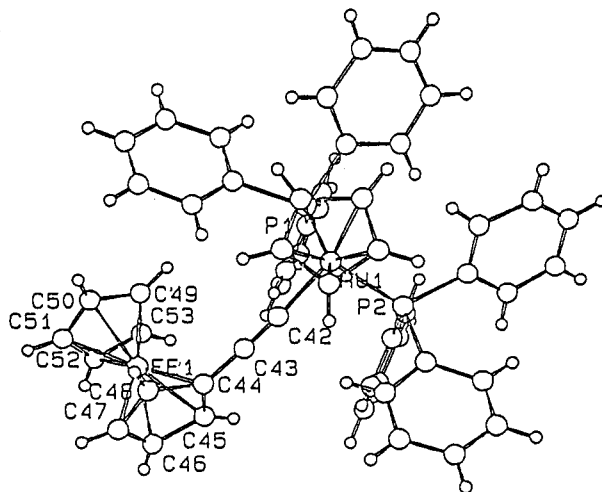(32) Raghavan, N. V.; Davis, R. E. *J. Cryst. Mol. Struct.* **1976**, *6*, 73.

(33) Bruce, M. I. *Pure Appl. Chem.* **1986**, *58*, 553.

(34) Nast, R. *Coord. Chem. Rev.* **1982**, *47*, 89.

Table 3. Positional Parameters and B_{eq} Values ($Å^2$) for 12

atom	x	y	z	B(eq)
Ru(1)	0.5479(1)	0.0257(2)	0.69153(9)	2.2(1)
Fe(1)	0.5980(2)	−0.2090(3)	0.9319(2)	3.0(2)
P(1)	0.4842(4)	0.1371(5)	0.7494(3)	2.4(3)
P(2)	0.4418(4)	−0.0733(5)	0.6387(3)	2.7(3)
P(3)	0.1401(4)	0.0201(9)	0.0997(3)	4.2(4)
F(1)	0.2205(8)	0.025(1)	0.1486(6)	5.8(8)
F(2)	0.135(1)	0.149(1)	0.1017(8)	7(1)
F(3)	0.145(1)	−0.109(1)	0.097(1)	9(1)
F(4)	0.0874(9)	0.010(1)	0.1493(7)	7(1)
F(5)	0.1906(8)	0.030(2)	0.0480(7)	8(1)
F(6)	0.0590(9)	0.018(2)	0.0488(7)	10(1)
C(1)	0.549(1)	0.189(2)	0.821(1)	2.2(5)
C(2)	0.520(1)	0.279(2)	0.850(1)	3.4(6)
C(3)	0.569(2)	0.316(2)	0.904(1)	3.8(7)
C(4)	0.640(1)	0.270(2)	0.928(1)	2.8(6)
C(5)	0.665(1)	0.183(2)	0.897(1)	3.3(6)
C(6)	0.621(1)	0.140(2)	0.844(1)	3.6(6)
C(7)	0.449(1)	0.266(2)	0.710(1)	2.0(5)
C(8)	0.377(1)	0.267(2)	0.665(1)	3.3(6)
C(9)	0.357(2)	0.364(2)	0.633(1)	4.7(7)
C(10)	0.405(2)	0.450(2)	0.642(1)	5.7(7)
C(11)	0.474(2)	0.454(3)	0.680(1)	7.2(9)
C(12)	0.499(2)	0.359(2)	0.715(1)	4.5(7)
C(13)	0.399(1)	0.093(2)	0.782(1)	2.6(5)
C(14)	0.401(1)	−0.005(2)	0.8103(9)	2.6(5)
C(15)	0.343(1)	−0.041(2)	0.841(1)	3.7(6)
C(16)	0.282(1)	0.027(2)	0.840(1)	3.3(5)
C(17)	0.276(1)	0.126(2)	0.815(1)	4.0(6)
C(18)	0.336(1)	0.163(2)	0.787(1)	3.3(6)
C(19)	0.372(1)	−0.005(2)	0.579(1)	3.4(6)
C(20)	0.391(1)	0.097(2)	0.557(1)	3.8(6)
C(21)	0.338(2)	0.148(2)	0.508(1)	4.3(6)
C(22)	0.267(1)	0.109(2)	0.486(1)	3.6(6)
C(23)	0.247(1)	0.008(2)	0.509(1)	3.9(6)
C(24)	0.298(1)	−0.050(2)	0.554(1)	3.2(6)
C(25)	0.373(1)	−0.149(2)	0.679(1)	1.9(5)
C(26)	0.391(1)	−0.254(2)	0.700(1)	3.2(6)
C(27)	0.338(2)	−0.309(2)	0.731(1)	4.6(7)
C(28)	0.269(2)	−0.258(2)	0.737(1)	3.8(6)
C(29)	0.253(2)	−0.157(2)	0.715(1)	5.1(7)
C(30)	0.303(1)	−0.099(2)	0.687(1)	3.2(6)
C(31)	0.478(1)	−0.187(2)	0.597(1)	2.4(5)
C(32)	0.544(1)	−0.247(2)	0.624(1)	2.7(6)
C(33)	0.572(1)	−0.336(2)	0.596(1)	4.4(7)
C(34)	0.533(1)	−0.368(2)	0.540(1)	3.5(6)
C(35)	0.466(1)	−0.313(2)	0.511(1)	3.6(6)
C(36)	0.437(1)	−0.226(2)	0.538(1)	3.2(6)
C(37)	0.679(2)	0.054(2)	0.701(1)	5.1(7)
C(38)	0.654(1)	−0.016(2)	0.651(1)	3.7(6)
C(39)	0.601(1)	0.052(2)	0.609(1)	2.7(6)
C(40)	0.591(1)	0.156(2)	0.633(1)	3.3(6)
C(41)	0.642(1)	0.154(2)	0.692(1)	2.8(6)
C(42)	0.564(1)	−0.094(2)	0.754(1)	2.8(6)
C(43)	0.582(1)	−0.163(2)	0.792(1)	2.4(5)
C(44)	0.603(1)	−0.240(2)	0.838(1)	2.0(5)
C(45)	0.550(1)	−0.314(2)	0.861(1)	3.2(6)
C(46)	0.598(2)	−0.372(2)	0.911(1)	4.1(7)
C(47)	0.674(1)	−0.334(2)	0.923(1)	3.7(6)
C(48)	0.680(1)	−0.249(2)	0.879(1)	3.5(6)
C(49)	0.551(2)	−0.054(2)	0.948(1)	4.8(7)
C(50)	0.631(1)	−0.066(2)	0.981(1)	3.8(6)
C(51)	0.632(1)	−0.151(3)	1.019(1)	6.3(8)
C(52)	0.557(2)	−0.200(3)	1.011(1)	6.2(8)
C(53)	0.508(2)	−0.145(3)	0.967(1)	6.3(8)

Figure 2. Molecular structure of 12.

Table 4. Selected Bond Distances and Bond Angles for Complex 12

Bond Distances (Å)			
Ru(1)–P(1)	2.293(7)	Ru(1)–P(2)	2.303(7)
Ru(1)–C(42)	1.99(2)	Ru(1)–C(37)	2.24(3)
Ru(1)–C(38)	2.25(2)	Ru(1)–C(39)	2.24(2)
Ru(1)–C(40)	2.26(2)	Ru(1)–C(41)	2.24(2)
Ru(1)–C(42)	1.99(2)	Fe(1)–C(44)	2.16(2)
Fe(1)–C(45)	2.08(2)	Fe(1)–C(46)	2.02(3)
Fe(1)–C(47)	2.03(2)	Fe(1)–C(48)	2.08(2)
Fe(1)–C(49)	2.10(3)	Fe(1)–C(50)	2.07(2)
Fe(1)–C(51)	2.06(3)	Fe(1)–C(52)	2.04(3)
Fe(1)–C(53)	2.02(3)	C(42)–C(43)	1.19(3)
C(43)–C(44)	1.38(3)	C(37)–C(38)	1.41(3)
C(37)–C(41)	1.36(3)	C(38)–C(39)	1.43(3)
C(39)–C(40)	1.40(3)	C(40)–C(41)	1.43(3)
C(44)–C(45)	1.44(3)	C(44)–C(48)	1.46(3)
C(45)–C(46)	1.44(3)	C(46)–C(47)	1.36(3)
C(47)–C(48)	1.44(3)	C(49)–C(50)	1.43(3)
C(49)–C(53)	1.43(3)	C(50)–C(51)	1.34(3)
C(51)–C(52)	1.40(3)	C(52)–C(53)	1.35(3)

Bond Angles (deg)			
P(1)–Ru(1)–P(2)	100.3(2)	P(1)–Ru(1)–C(42)	92.4(7)
P(2)–Ru(1)–C(42)	88.4(7)	C(37)–Ru(1)–C(42)	92.7(9)
C(38)–Ru(1)–C(42)	96.3(9)	C(39)–Ru(1)–C(42)	131.2(9)
C(40)–Ru(1)–C(42)	153.7(9)	C(41)–Ru(1)–C(42)	120.2(9)
Ru(1)–P(1)–C(1)	114.4(8)	Ru(1)–P(1)–C(7)	111.6(7)
Ru(1)–P(1)–C(13)	124.2(8)	C(1)–P(1)–C(7)	103(1)
C(1)–P(1)–C(13)	98.2(9)	C(7)–P(1)–C(13)	103(1)
Ru(1)–P(2)–C(19)	119.1(8)	Ru(1)–P(2)–C(25)	121.3(7)
Ru(1)–P(2)–C(31)	109.9(8)	C(19)–P(2)–C(25)	101(1)
C(19)–P(2)–C(31)	101(1)	C(25)–P(2)–C(31)	101(1)
Ru(1)–C(42)–C(43)	173(2)	C(42)–C(43)–C(44)	178(3)
C(43)–C(44)–Fe(1)	124.1(2)	C(45)–C(44)–C(48)	107(2)
C(44)–C(45)–C(46)	106(2)	C(45)–C(46)–C(47)	112(2)
C(46)–C(47)–C(48)	107(2)	C(44)–C(48)–C(47)	108(2)
C(50)–C(49)–C(53)	106(2)	C(49)–C(50)–C(51)	108(2)
C(50)–C(51)–C(52)	110(3)	C(51)–C(52)–C(53)	109(3)
C(49)–C(53)–C(52)	108(3)		

(i) the Fe—C(44) distance (2.16 Å) is extended more than other Fe—C distances (2.08, 2.08, 2.03, and 2.02 Å) of the substituted cyclopentadienyl (Cp) ring. The change of the Fe—C distances observed here may reflect the shortening of the C(46)—C(47) distance (1.38 Å) in the substituted Cp ring. (ii) The acetylide framework bends away by 5.5° from the mean plane of the substituted Cp ring of the ferrocenyl moiety toward the Fe atom. Such a great distortion of a ferrocene framework has been not yet reported at least in the ferrocenium cation derivatives,

to the best of our knowledge, although the extended bond length (2.154 Å) was observed in the bond between the Fe atom and the ipso-carbon atom of the substituted ferrocenyl ring in (η-$C_5H_4S)_2FePd(PPh_3$).[35] In the diphenyl-ferrocenylcarbenium cation in which a large contribution of the fulvenyl structure is assumed, it is reported[36] that the distances between the C atoms of the Cp ring and the Fe atom are 2.009(6), 2.060(8), 2.095(6), 2.085(8), and 2.018-(8) Å, and the C_α—C_{ipso} distance is 1.416(9) Å. Thus, the

(35) (a) Seyferth, D.; Hames, B. W.; Rucker, T. G.; Cowie, M.; Dickson, R. S., *Organometallics* **1983**, *2*, 472. (b) Cowie, M.; Dickson, R. S. *J. Organomet. Chem.* **1987**, *326*, 269.

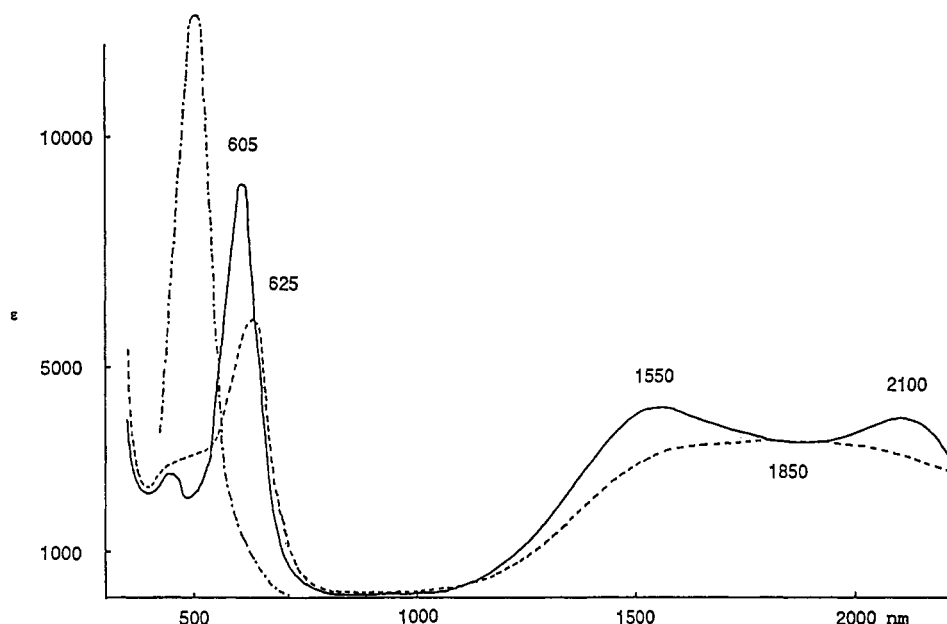(36) Behrens, U. *J. Organomet. Chem.* **1979**, *182*, 89.

Figure 3. Vis–NIR spectra of **12** (—) and **14** (- - -) in CH_2Cl_2.

Table 5. Visible and Near-Infrared Spectral Data for the Oxidized Complexes 12–14

complex	solvent	$1/n^2 - 1/D_s{}^a$	$10^{-3}\nu_{max}$, cm^{-1} $(\epsilon)^b$
12	CH_2Cl_2	0.380	22.7 (2740), 16.6 (8800), 6.34 (4080), 4.75 (2460)
	CH_3NO_2	0.489	23.5 (3200), 17.0 (8130), 6.61 (3930), 4.66 (1840)
	CH_3CN	0.526	23.5 (3100), 17.0 (8110), 6.62 (3990), 4.68 (1820)
	CD_3CN	0.528	23.8 (3170), 17.1 (8340), 6.62 (4020), 4.76 (1730)
13	CH_2Cl_2	0.380	23.0 (2620), 16.7 (5140), 6.48 (2100), 4.49 (1830)
14	CH_2Cl_2	0.380	21.5 (3000),^{c} 16.0 (5980), 6.27 (3060), 4.82 (1900)

^{a} From ref 3d. ^{b} The bands at a near-infrared region were peak-separated as two Gausian peaks. ^{c} Shoulder.

crystal data confirm the great contribution of the limiting structures **B**, other than the limiting structure **A**, in the oxidized complex **12**. Consequently, the X-ray analytical datum of **12** supports the suggestion from the IR spectra that there is a large electron delocalization between the Ru and Fe atoms in the oxidized complexes **12–14**.

The one-electron-oxidized complexes **12–14** showed broad absorptions in the near-infrared region. The vis–NIR (NIR = near-infrared) spectra of **12** and **14** are shown in Figure 3, and their spectral data are summarized in Table 5, along with those for **13**. A similar absorption in the near-infrared region is also reported in oxidized $FcCNRu(NH_3)_5$ (1100 nm)[9] and $FcCCo_3(CO)_6L_3$ (L = P(OPh)$_3$, 1545 nm)[10] and assigned as an intervalence transition (IT) band. In the Fe analogs **15**, a similar intervalence band was also observed at 1500–1600 nm.[37] So, the low-energy electronic band near 1600 nm would be assigned to the intervalence transition involving light-induced electron transfer between the dissimilar ferrocene and Ru(III) nuclei, although the assignment to another near-infrared absorption near 2200 nm is uncertain at the present. The appearance of the IT band in the near-infrared spectra of the mixed-valence complexes, **12–14**, would further support the presence of electron delocal-

ization between the dissimilar metal centers. The absorption maximum of the low-energy band showed only a little linear dependence on $(1/n^2 - 1/D_s)$, where n^2 and D_s are the optical and static dielectric constants of the solvent involved.[4c] Meyer described that the system which involved delocalized iron sites, for example, the [0.0]-ferrocenophane monocation, is relatively insensitive to changes in solvent.[4c] Application of Hush's theoretical analysis[38] of intervalence-transfer (IT) transition to complex **12** is of some interest. In the treatment the half-width $(\Delta\nu_{1/2})$ is related to the energy of the IT transition (ν_{max}) by the equation

$$\nu_{max} - \nu_0 = (\Delta\nu_{1/2})^2/2310 \text{ (cm}^{-1})$$

where ν_0 is the internal energy difference between the two oxidation-state isomers. According to Taube's treatment in oxidized $FcCNRu(NH_3)_5$,[9a] the value of ν_0 can be estimated to an upper limit by the difference in the redox potentials of the two centers in the molecule. For **12**, the difference in potentials is obtained to be 0.60 V (ν_0 = 4.8 $\times 10^3$ cm^{-1}) from the cyclic voltamogram (Table 1). With the use of the above equation, a lower limit of 1.9 $\times 10^3$ cm^{-1} (in CH_2Cl_2) is calculated for $\Delta\nu_{1/2}$ (calcd), while the corresponding observed value $\Delta\nu_{1/2}$ (obsd) is 3.8 $\times 10^3$ cm^{-1}. The ratio between observed and calculated $\Delta\nu_{1/2}$ (2.0) is considerably larger than that (1.1–1.3) reported for mixed-valence compounds of a type of class II.[10] Hush further proposed[38] an expression for the interaction parameter α^2 which gives an approximate measure of the degree of ground-state delocalization in a mixed-valence complex, where d is the distance separating the metal center.

$$\alpha^2 = [(4.2 \times 10^{-4})\epsilon_{max}\Delta\nu_{1/2}]/\nu_{max}d^2$$

Using the internuclear separation obtained from the X-ray analysis (6.009(5) Å), a value for α^2 of 2.8 $\times 10^{-2}$ (in CH_2-Cl_2) is calculated for the oxidized complex **12**. The value obtained is much larger than the values of α^2 for several class II mixed-valence ions: diferrocenylacetylene monocation (**16**) (2.4 $\times 10^{-3}$),[4d] [$(NH_3)_5RuNCFc$]$^+$ (2.3 $\times 10^{-3}$),[9a] [$FcCCo_3(CO)_6L_3$]$^+$ (2.7 $\times 10^{-3}$).[10] The value for **12** is still

(37) Sato, M.; Hayasi, Y.; Katada, M.; Kawata, S. *J. Organomet. Chem.*, in press.
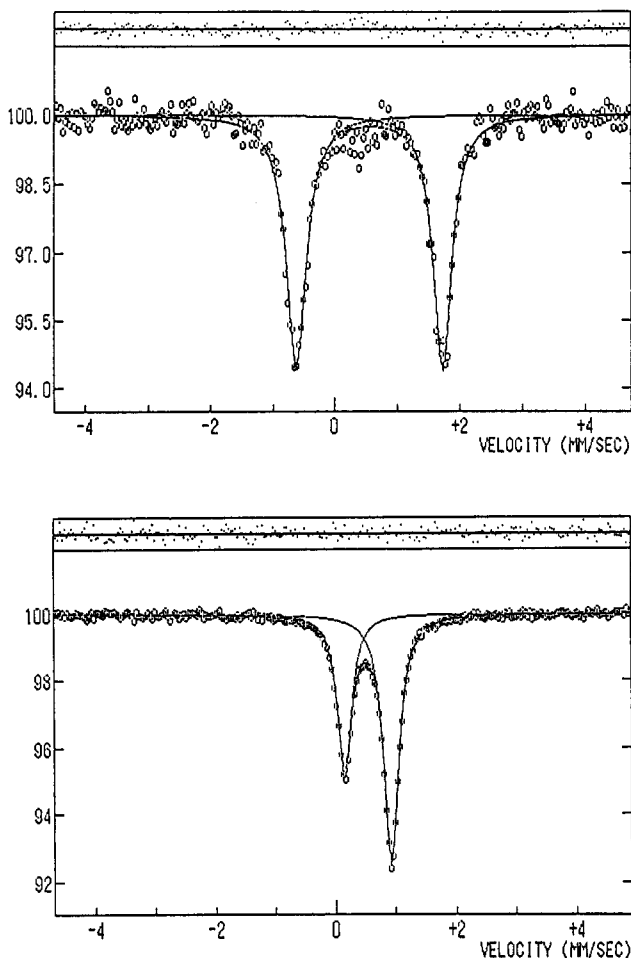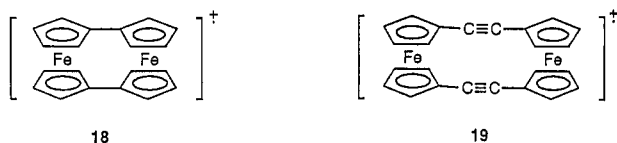
(38) Hush, N. S. *Prog. Inorg. Chem.* **1967**, *8*, 391.

Figure 4. Mössbauer spectra of **5** (upper) and **12** (bottom) at 78 K.

temperature independent. This asymmetry is assumed to arise from preferential crystal orientation. The Mössbauer spectra of ferrocenium and ferrocenyl groups are characterized by small or vanishing quadrupole splittings. The QS value for the ferrocenium part in the biferrocene monocation (**17**) and the differrocenylacetylene monocation (**16**), which are classified as class II mixed-valence ions, is, however, comparably large (0.288 mm s⁻¹ for **17** and 0.49 mm s⁻¹ for **16**).[4b] Also, in the chalcogen-substituted ferrocenium ion, the large QS values (0.495–0.84 mm s⁻¹) are observed.[39,40] It is, therefore, probably reasonable that the oxidized site in complex **12** is assigned to the iron atom of the ferrocenyl moiety. The large QS value (0.77 mm s⁻¹) in complex **12** seems to be induced from the good electron delocalization through the acetylide bond from the Ru(II) part of the complex. The oxidized complex **12** (probably also **13** and **14**) is, therefore, considered to be a well electron-delocalized class II type of heterobinuclear mixed-valence complex, since the QS value observed in **12** is much smaller than that in the class III mixed-valence ions, the [0.0]ferrocenophane (**18**) (QS = 1.78 mm s⁻¹) and [2.2]ferrocenophane-1,13-diyne monocations (**19**) (1.61 mm s⁻¹),[4b] the values of which are close to the averaged value between the Fe^{II}Fe^{II} and Fe^{III}Fe^{III} species.

Experimental Section

Visible and near-infrared spectra were recorded on a Shimadzu 365 spectrophotometer. Infrared spectra were recorded on a Hitachi 270-50 spectrophotometer, and ¹H and ¹³C NMR spectra, on a Bruker AM 400 spectrometer. Electrochemical measurements were made by cyclic voltammetry in a solution of 0.1 M tetrabutylammonium perchlorate in dichloromethane under nitrogen at 25 °C, using a standard three-electrode cell. All potentials were measured vs a Ag/AgNO₃ (0.05 M) electrode, and the scan rate was 100 mV/s.

Ferrocenylacetylene (FcCCH) was prepared from acetylferrocene according to the literature.[41] Cp(dppf)RuCCFc (**6**) was prepared by a procedure described previously.[42] (η-C₅H₅)(Ph₃P)₂-RuCl (**1**),[43] (η-C₅H₅)(dppe)RuCl (**2**),[44] (η-C₅Me₅)(Ph₃P)₂RuCl,[45] and (η-C₅Me₅)(dppe)RuCl[45] were prepared according to the procedure described in the literature.

Cp(Ph₃P)₂RuCCFc (4). To a solution of (NH₄)PF₆ (21 mg, 0.1 mmol) in MeOH (3 mL) was added a solution of (η-C₅H₅)(Ph₃P)₂RuCl (72.6 mg, 0.1 mmol) in dichloromethane (5 mL) and subsequently FcCCH (21 mg, 0.1 mmol) under bubbling of N₂. The solution was stirred for 1 h at room temperature. To the solution was added a solution of sodium methoxide in methanol. The resulting yellow precipitates were collected by filtration and recrystallized from dichloromethane/methanol to yield orange-yellow crystals (87 mg, 97 %), mp 203 °C. IR (KBr): 2072 cm⁻¹. ¹H NMR (CD₂Cl₂): δ 3.70 (s, 5H, CpFe), 4.02 (s, 2H, Fc), 4.16 (s, 2H, Fc), 4.26 (s, 5H, CpRu), 7.13–7.49 (m, 30H, Ph). ¹³C NMR (CD₂Cl₂): δ 66.47 (Fc), 69.27 (CpFe), 69.64 (Fc), 76.82 (Fc-ipso), 85.55 (CpRu), 127.60 (Ph-*m*), 128.87 (Ph-*p*), 134.33 (Ph-*o*), 139.63 (t, J = 21.6 Hz, Ph-ipso). Anal. Calcd for C₅₃H₄₄P₂FeRu: C, 70.74; H, 4.92. Found: C, 70.73; H, 5.03.

Cp(dppe)RuCCFc (5): red-orange crystals (48 mg, 62%); mp 214–215 °C; IR (KBr) 2076 cm⁻¹; ¹H NMR (CD₂Cl₂) δ 2.39

larger than that of the directly coupled system, biferrocene monocation (**17**) (0.9 × 10⁻²–1.4 × 10⁻²),[2c] but smaller than that of the [0.0] ferrocenophane monocation (**18**) (4.5 ×

18   **19**

10⁻²–5.1 × 10⁻²) which is classified as a class III mixed-valence complex.[3a] Considering the effect of the distance between the two redox sites [α^2(FcC≡CFc⁺)/α^2(Fc—Fc⁺) = ca. 1/3], the observed value of α^2 for **12** may correspond to that for **18**. Such a large value of α^2 in complex **12** seems to be related to the electron delocalization between the two metal sites. An increased orbital overlapping between the redox sites compared with other systems may be largely responsible for the large electron delocalization observed in complex **12**. That is, an efficient dπ–pπ conjugation would be possible between the Ru atom and the acetylene group in **12**.

The Mössbauer spectrum of **12** is shown in Figure 4, along with that of the neutral complex **5**. The isomer shift (IS) and quadrupole splitting (QS) values of 0.55 and 2.42 mm s⁻¹, respectively, in complex **5** are typical for neutral ferrocene derivatives. In the Mössbauer spectrum of **12**, on the other hand, one doublet with the QS value of 0.77 mm s⁻¹ and the IS value of the 0.54 mm s⁻¹ was observed at 78 K. The relative intensity of the two components of the quadrupole doublet in complex **12** was

(39) Kramer, J. A.; Herbstein, F. H.; Hendrickson, D. N. *J. Am. Chem. Soc.* **1980**, *102*, 2293.

(40) Sato, M.; Katada, M.; Nakashima, S.; Sano, H.; Akabori, S. *J. Chem. Soc., Dalton Trans.* **1990**, 1979.

(41) Rosenblum, M.; Brawn, N.; Papenmeier, J.; Applebraum, M. *J. Organomet. Chem.* **1966**, *6*, 173.

(42) Sato, M.; Sekino, M. *J. Organomet. Chem.* **1992**, *444*, 185.

(43) Bruce, M. I.; Windsor, N. J. *Aust. J. Chem.* **1977**, *30*, 1601.

(44) Ashby, G. S.; Bruce, M. I.; Tomkins, I. B.; Wallis, R. C. *Aust. J. Chem.* **1979**, *32*, 1003.

(45) Oshima, N.; Suzuki, H.; Moro-oka, Y. *Chem. Lett.* **1984**, 1161.

(m, 2H, CH$_2$), 2.82 (m, 2H, CH$_2$), 3.64 (s, 5H, CpFe), 3.48 (t, J = 1.7 Hz, 2H, Fc), 3.71 (t, J = 1.8 Hz, 2H, Fc), 4.72 (s, 5H, CpRu), 7.13–7.49 (m, 20H, Ph); ^{13}C NMR (CD$_2$Cl$_2$) δ 27.98 (t, J = 23.3 Hz, CH$_2$), 66.12 (Fc), 68.85 (CpFe), 69.14 (Fc), 76.02 (Fc-ipso), 82.45 (CpRu), 127.68, 127.72 (Ph-m), 128.00, 128.91 (Ph-p), 131.62, 134.32 (Ph-o), 137.82, 143.01 (m, Ph-ipso). Anal. Calcd for C$_{43}$H$_{38}$P$_2$FeRu: C, 66.75; H, 4.95. Found: C, 66.58; H, 5.05.

Cp*(Ph$_3$P)$_2$RuCCFc (7): red-brown crystals (52 mg, 54%); mp 140 °C dec; IR (KBr) 2068 cm^{-1}; ^{1}H NMR (CDCl$_3$) δ 1.19 (s, 15H, CH$_3$), 4.09 (s, 7H, Fc + CpFe), 4.32 (s, 2H, Fc), 7.06–7.56 (m, 30H, Ph); ^{13}C NMR (CD$_2$Cl$_2$) δ 11.71 (CH$_3$), 68.88 (Fc), 71.14 (Fc), 71.39 (CpFe), 79.65 (ipso-Fc), 95.60 (C$_5$Me$_5$), 129.13 (p-Ph), 130.56 (Ph-m), 137.17 (Ph-o), 140.12 (Ph-ipso). Anal. Calcd for C$_{58}$H$_{54}$P$_2$FeRu: C, 71.82; H, 5.61. Found: C, 71.94; H, 5.75.

Cp*(dppe)RuCCFc (18): deep-orange crystals (64 mg, 77%); mp 160 °C dec; IR (KBr) 2080 cm^{-1}; ^{1}H NMR (CDCl$_3$) δ 1.57 (s, 15H, CH$_3$), 2.05 (m, 2H, CH$_2$), 2.75 (m, 2H, CH$_2$), 3.82 (s, 7H, Fc–CpFe), 3.86 (s, 2H, Fc), 7.20–7.84 (m, 20H, Ph); ^{13}C NMR (CD$_2$Cl$_2$) δ 10.24 (CH$_3$), 29.76 (t, J = 23.3 Hz), 66.16 (Fc), 69.14 (CpFe), 69.41 (Fc), 77.26 (Fc-ipso), 92.57 (C$_5$Me$_5$), 103.45 (Fc–C–), 120.31 (Ru–C–), 127.43, 127.77 (d, J = 1.9 Hz, Ph-m), 129.16 (s, Ph-p), 133.51, 134.44 (d, J = 5.2 Hz, Ph-o), 137.65 (d, J = 43.2 Hz, Ph-ipso), 139.53 (m, Ph-ipso). Anal. Calcd for C$_{48}$H$_{48}$P$_2$FeRu: C, 68.33; H, 5.73. Found: C, 68.15; H, 5.77.

[Cp(Ph$_3$P)$_2$RuCCFc]PF$_6$ (12). To a solution of Cp(Ph$_3$P)$_2$-RuCCFc (90 mg, 0.1 mmol) in dichloromethane (1 mL) and benzene (10 mL) was added ferrocenium hexafluorophosphate (33 mg, 0.1 mmol) under bubbling N$_2$ on an ice bath. The mixture was stirred for 4 h. The resulting blue-violet precipitates were filtered. The precipitates were recrystallized from dichloromethane/hexane to give dark blue needles (95 mg, 91%), mp 182 °C. IR (KBr): 1986 cm^{-1}. Vis–NIR (CH$_2$Cl$_2$): 450 (ϵ 2740), 610 (8800), 1575 (4030), 2100 nm (3790). Anal. Calcd for C$_{53}$H$_{44}$P$_3$F$_6$FeRu: C, 60.97; H, 4.22. Found: C, 60.93; H, 4.24.

[Cp(dppf)RuCCFc]PF$_6$ (13): dark blue needles (99 mg, 92%); mp 173.5 °C; IR (KBr) 1972 cm^{-1}; Vis–NIR (CH$_2$Cl$_2$) 435 (ϵ 2620), 600 (5140), 1570 (2350), 2060 nm (2300). Anal. Calcd for C$_{51}$H$_{42}$P$_3$Fe$_2$Ru: C, 57.01; H, 3.94. Found: C, 56.95; H, 4.06.

[Cp*(Ph$_3$P)$_2$RuCCFc[PF$_6$ (14): black crystals (102 mg, 93%); mp 140 °C dec; IR (KBr) 1978 cm^{-1}; Vis–NIR (CH$_2$Cl$_2$) 460 sh (ϵ 3000), 625 (5970), 1850 nm (3300). Anal. Calcd for C$_{58}$H$_{54}$P$_3$F$_6$FeRu·CH$_2$Cl$_2$: C, 59.09; H, 4.70. Found: C, 58.83; H, 4.81.

Mössbauer Spectroscopic Measurements. Mössbauer spectroscopic experiments were carried out by using a constant acceleration-type spectrometer. The temperature of the absorb-ers was kept within ±0.5 K. The spectra observed were fitted with Lorentzian line shapes by using the least-squares fitting procedure. The velocity scale was calibrated by using a metallic iron-foil spectrum. The isomer shifts were reported with respect to α-Fe foil at room temperature. The error of the values of the isomer shift and quadrupole splitting was estimated to be approximately within ±0.02 mm s^{-1}.

Structure Determination. Crystal data for 12: C$_{53}$H$_{44}$P$_3$F$_6$-RuFe, fw = 1044.76, monoclinic, $P2_1/a$; a = 17.176(9), b = 12.055-(7), c = 22.480(9) Å^3; β = 101.35(4)°; V = 4563(4) Å^3; Z = 4; D_{calc} = 1.520 g/cm^3; μ(Mo Kα) = 8.05 cm^{-1}; T = 296 K; crystal size 0.100 × 0.030 × 0.100 mm.

All measurements were made on a Rigaku AFC5R diffracto-meter with graphite monochromated Mo Kα radiation and a 12-kW rotating anode generator. The data were collected at a temperature of 23 °C using the $\omega/2\theta$ scan technique to a maximum 2θ value of 45.0°. Cell parameters for data collection were obtained from a least-squares refinement using the setting angles of 15 carefully centered reflections in the range 8.56 < 2θ < 23.45°. During data collection three standards (measured before every 200 reflections) showed no significant variation. Of 5255 independent reflections measured, only 4792 were considered as being observed on the basis of the criterion F_o > 2σ(F_o). Azimuthal scans of several reflections indicated no need for an absorption correction. The data were corrected for Lorentz and polarization effects.

The structure was solved by direct methods. The non-hydrogen atoms were refined either anisotropically or isotropi-cally. The final cycle of full-matrix least-squares refinement was based on 1462 observed reflections with I > 3.00σ(I) and 313 variable parameters and converged with unweighted and weighted agreement factors of R = 0.57 and R_w = 0.56. The standard deviation of an observation of unit weight was 1.23.

Supplementary Material Available: Tables of crystal data, positional parameters, bonding distances, bond angles, and anisotropic thermal parameters and a figure giving the structure of 12 (15 pages). Ordering information is given on any current masthead page.

OM930242Q